DOI 10.1007/s11182-019-01851-4

Russian Physics Journal, Vol. 62, No. 8, December, 2019 (Russian Original No. 8, August, 2019)

EVOLUTION OF THE STRUCTURAL-PHASE STATE OF A TITANIUM ALLOY OF THE SYSTEM Ti–Al–V–Mo DURING FORMATION OF AN ULTRAFINE-GRAINED STRUCTURE USING REVERSIBLE HYDROGENATION

G. P. Grabovetskaya,[1] O. V. Zabudchenko,[1] I. P. Mishin,[1] E. N. Stepanova,[2] I. V. Ratochka,[1] and O. N. Lykova[1]

UDC 539.42:539.382

Using methods of electron-microscopy and x-ray structural analysis, we have investigated peculiarities of the evolution of the structural-phase state of an alloy of the system Ti–Al–V–Mo *during formation of an ultrafine-grained structure by a method combining hot plastic deformation and reversible hydrogenation. It has been shown that the presence in solid solution of 0.15 wt% hydrogen makes it possible to lower by more than a factor of 2 the magnitude of the plastic deformation needed to obtain an ultrafine-grained state in the alloy. We found that during deformation and subsequent degassing of hydrogen from the alloy, such processes as the phase transformations* $\alpha'' \rightarrow \beta \rightarrow \alpha$ *and* $\beta \rightarrow \alpha''$ *and a redistribution of the doping elements take place, facilitating the formation of a lamellar morphology in the grains and preservation of a high level of strength properties of the ultrafine-grained structure.*

Keywords: titanium alloy, hydrogen, ultrafine-grained structure, phase transformation.

INTRODUCTION

Two-phase titanium alloys (of α+β-type) comprise about 90% of the titanium alloys used at the present time in industry. The mechanical properties of these alloys depend substantially on their microstructure and phase composition. An effective way of enhancing the mechanical properties of titanium alloys is to create an ultrafine-grained (UFG) state in them by methods of severe plastic deformation (SPD) [1–3]. At the present time, it has been established that in the formation of the UFG state in alloys, including titanium alloys, such processes as formation of supersaturated solid solutions and phase transformations at nonequilibrium temperatures can take place [4–8]. This fact can be used to obtain a UFG state containing two or several structural elements (or phases) of different degrees of dispersion with the aim of providing a combination of required properties of the alloy [6, 9]. Toward this same end, it is possible to use preliminary (prior to SPD) hydrogenation of the titanium alloys. It is well known that the presence of hydrogen has a substantial effect on structural-phase transformations in titanium alloys during deformation, and this fact is used in the thermal-hydrogen treatment of titanium alloys with the goal of altering their structure and properties [10–12]. However, after being put into use, the presence of hydrogen can give rise to embrittlement and premature failure of parts made from titanium alloys [13]. Therefore, the concluding operation of thermal-hydrogen treatment of titanium alloys is degassing of the alloy by annealing in vacuum at elevated temperatures, which can also lead to a change in the structure and phase composition of the alloys. The majority of studies of the regularities of formation of the UFG structure of

[1]Institute of Strength Physics and Materials Science, Siberian Branch of the Russian Academy of Sciences, Tomsk, Russia, e-mail: grabg@ispms.tsc.ru; lekalune@mail.ru; mip@ispms.tsc.ru; ivr@ispms.tsc.ru; lon8@yandex.ru; [2]National Research Tomsk Polytechnic University, Tomsk, Russia, e-mail: enstepanova@tpu.ru. Translated from Izvestiya Vysshikh Uchebnykh Zavedenii, Fizika, No. 8, pp. 21–27, August, 2019. Original article submitted April 17, 2019.

titanium alloys during SPD in the presence of hydrogen were previously carried out on (α+β)-titanium alloys with a small volume fraction of the β-phase [10–12]. At the same time, for alloys with a large volume fraction of the β-phase the formation of the UFG structure in the presence of hydrogen can have its own peculiarities.

The aim of the present work is to investigate the formation of the UFG structure in a titanium alloy of the Ti–Al–V–Mo–H system by pressing with a change of the deformation axis and subsequent degassing.

MATERIALS AND METHODS OF STUDY

As the material for study, we chose an (α+β)-titanium alloy of the system Ti–Al– V–Mo–H with content of the main doping elements 3.1 Al – 4.5 V – 4.9 Mo wt%. In its initial state, the alloy is coarse-grained and contains 0.002 wt% hydrogen (in what follows, the alloy VT16). Hydrogenation of the alloy to roughly 0.15 wt% (in what follows, the alloy VT16-0.15H) was performed by annealing in a hydrogen medium in a high-vacuum Sieverts-type device (PCIM) at 873 K. The hydrogen concentration in the alloy was measured with the help of a RHEN 602 analyzer with an accuracy of 0.0001%.

The UFG structure in the VT16 and the VT16-0.15H alloys was formed by pressing with a change of the deformation axis and gradual lowering of the temperature in the interval 1023–723 K. Pressing of the alloys was performed in two and five cycles. One cycle consisted of three pressings. Deformation during one pressing was ~50%. Pressing was performed at the rate of $\sim 10^{-3}$ s^{-1}. Before pressing, the VT16 alloy was quenched from a temperature of 1068 K, and the VT16-0.15H alloy, from a temperature of 923 K.

The structure of the alloys was investigated with the help of an AXIOVERT-200MAT optical microscope and a JEM-2100 transmission electron microscope. The sizes of the structural elements of the alloys in the UFG state were determined by the secant method on photographs of the dark-field image of the microstructure. The sample consisted of not less than 180 elements. The phase composition and lattice parameters of the phases of the alloy were determined by standard methods of x-ray structural analysis with the help of a Shimadzu XRD-7000 diffractometer with CuK_α radiation. We used the software package PowderCell to decipher the diffraction patterns.

Tension tests were conducted at room temperature (293 K) on a PV-3012M machine with automatic recording of the tension curve in load–time coordinates. The initial tension rate was $6.9 \cdot 10^{-3}$ s^{-1}. Dumb-bell test pieces with gage sections of 5×1.5×0.7 mm were cut from billets by the electrospark technique. The surfaces of the specimens were subjected to mechanical grinding and electrolytic polishing before testing.

RESULTS AND DISCUSSION

The investigated VT16 alloy in its as-delivered (initial) state has a polycrystalline structure with average grain size ~27 μm and contains two phases: α and β. The β-phase content in the alloy comprises (22 ± 1) vol.%. Hydrogenation of VT16 alloy at 873 K to a concentration of 0.15 wt% H does not change the average grain size, but increases the volume fraction of the β-phase to (26 ± 1) vol.%. As a result of quenching from 923 K, a three-phase (α + α″ + β) laminar structure is formed in the VT16-0.15H alloy with a transverse size of the platelets equal to 0.5–1.5 μm (Fig. 1*a*). A typical segment of the diffraction pattern of such a structure is shown in Fig. 1*b*. In the VT16 alloy, an analogous three-phase laminar structure is formed only after quenching from 1068 K [6].

X-ray structural analysis showed that during pressing in both quenched alloys, a gradual decay of the α″-phase takes place according to the scheme α″→β→α. After two pressing cycles at 1023 K and 923 K, both alloys become two-phase and contain the α-phase and the β-phase (Fig. 2, curves *1* and *3*). The volume fraction of the β-phase in the VT16 and VT16-0.15H (wt% H) alloys after two pressing cycles was 35 vol.% and 42 vol.%, respectively. The increase in the volume fraction of the β-phase in the alloys in comparison with the initial state (~22 vol.%) leads to a decrease in the content of doping elements in its volume. This is attested by an increase in the lattice parameters of the β-phase in the indicated alloys up to 0.3252 nm and 0.3261 nm, respectively, in comparison with the initial state (0.3245 nm). (It is well known that the lattice parameters of the β-phase in the VT16 alloy increase with decrease of the concentration of the doping elements in its volume [14].) After two pressing cycles, the magnitude of the elastic microdistortions of the

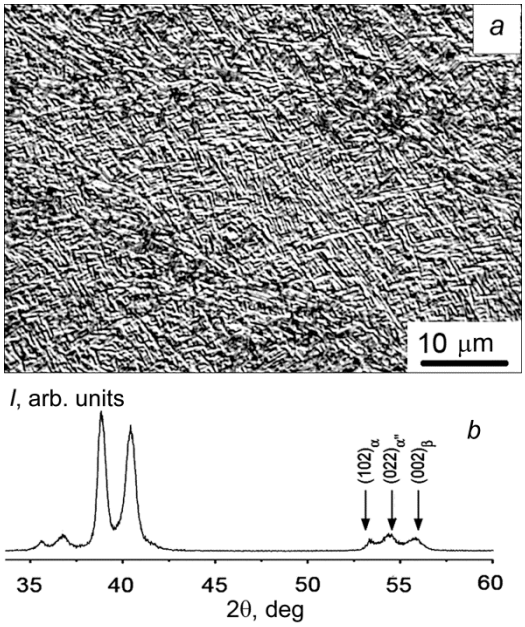

Fig. 1. Microstructure (*a*) and segment of the diffraction pattern (*b*) of the alloy VT16-0.15H, quenched from 923 K.

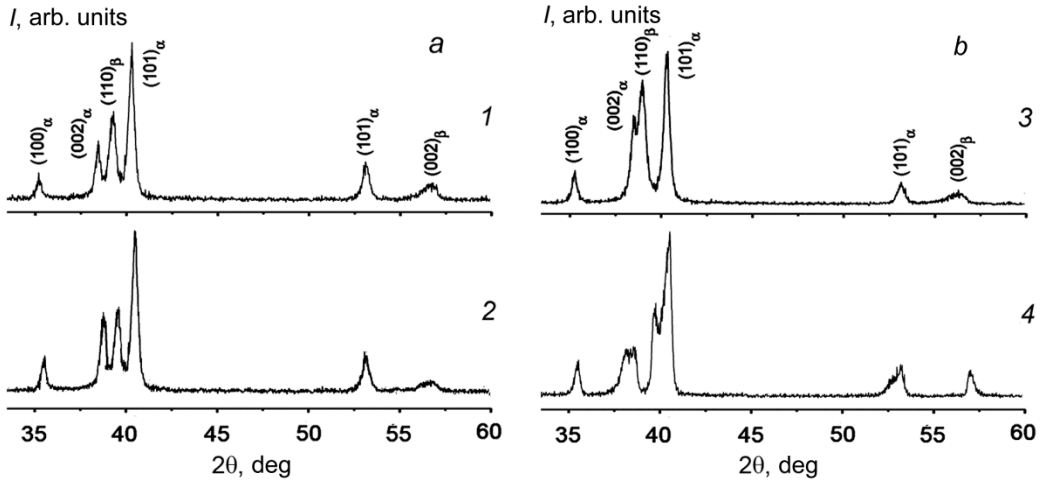

Fig. 2. Segments of a diffraction pattern of the alloys VT16 (*a*) and VT16-0.15H (*b*): curves *1* and *3* are for the state after two pressing cycles, curve *2* is for the VT16 alloy in the state after five pressing cycles, and curve *4* is for the VT16-0.15H alloy in the state after hydrogen degassing.

crystalline lattices of the α- and β-phases in the VT16 alloy was $1.2 \cdot 10^{-3}$ and $1.9 \cdot 10^{-3}$, respectively. In the VT16-0.15H alloy, the magnitude of the microdistortions of the crystalline lattices of the α- and β-phases is somewhat higher ($1.5 \cdot 10^{-3}$ and $2.2 \cdot 10^{-3}$, respectively), which apparently is due to the presence of hydrogen in solid solution. In the VT16 alloy in the initial state, the magnitude of the microdistortions of the crystalline lattices of the α- and β-phases did not exceed 10^{-4}.

In the VT16 alloy after two pressing cycles at 1023 K and 923 K, a UFG grain-subgrain structure with average size of the elements (0.45 ± 0.16) μm is formed. Further pressing up to five cycles with gradual lowering of the

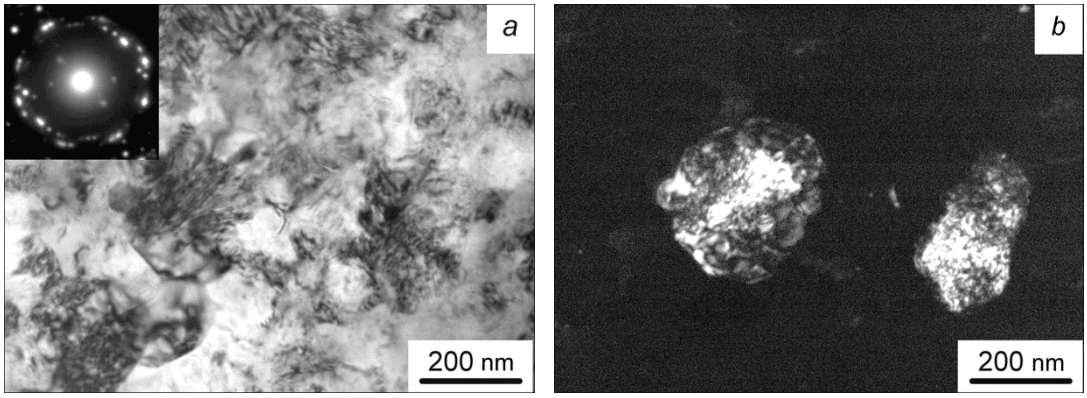

Fig. 3. Electron-microscope image of the microstructure of the VT16 alloy after five pressing cycles: *a*) bright-field image and microdiffraction pattern, *b*) dark-field image in the [100]α reflection.

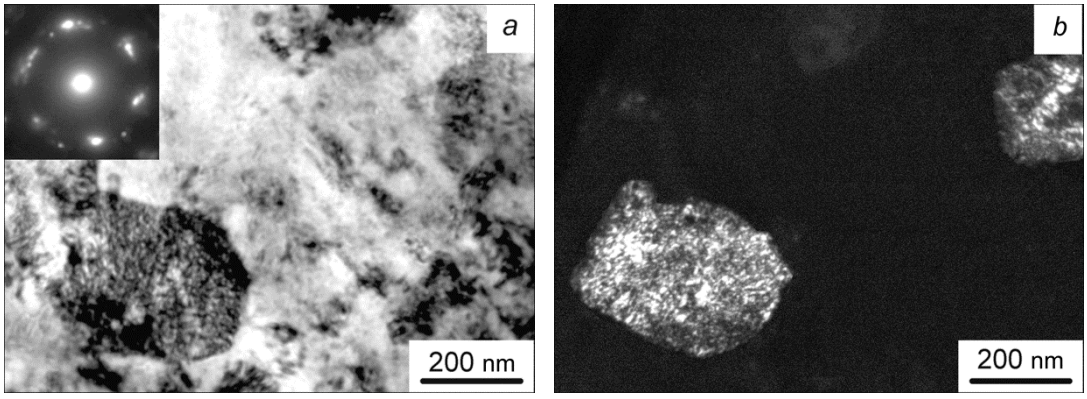

Fig. 4. Electron-microscope image of the microstructure of the VT16-0.15H alloy after two pressing cycles: *a*) bright-field image and microdiffraction pattern, *b*) dark-field image in the [100]α reflection.

temperature to 723 K leads to an increase in the degree of dispersion of the UFG structure of the VT16 alloy, a typical electron-microscope image of which is shown in Fig. 3. In the bright-field image of this structure (Fig. 3*a*), grain boundaries and individual dislocations are not manifested. The presence in a unit volume of the structure of a large number of elements and substantial misorientation between them is attested by the significant number of reflections, uniformly spaced around a circle, in the electron diffraction pattern taken from an area of 1.5 μm^2 (Fig. 3*a*). The average size of the elements of the UFG grain-subgrain structure of the VT16 alloy, determined from the dark-field image, is (0.23 ± 0.19) μm.

X-ray structural analysis of the UFG structure of the VT16 alloy showed that during pressing at temperatures of 873 K, 823 K, and 773 K, a β→α phase transformation takes place (Fig. 2, curve *2*). The volume fraction of the β-phase is decreased roughly from 35% to 30%, and its lattice parameter, from 0.3252 nm to 0.3249 nm. The magnitudes of the microdistortions of the crystalline lattices of the α- and β-phases of the UFG structure obtained as a result of five pressing cycles increase to $3.5 \cdot 10^{-3}$ and $3 \cdot 10^{-3}$, respectively.

In the VT16-0.15H alloy, during two pressing cycles at 1023 K and 932 K, a UFG uniform grain-subgrain structure is also formed. An electron-microscope image of the UFG structure of the VT16-0.15H alloy is shown in Fig. 4. The complex deformational contrast and high internal stresses do not allow the features of the microstructure to be manifested in the bright-field image of the UFG structure of the VT16-0.15H alloy (Fig. 4*a*). At the same time, it can be clearly seen in the dark-field image that the structure of the alloy consists of individual elements (Fig. 4*b*). The

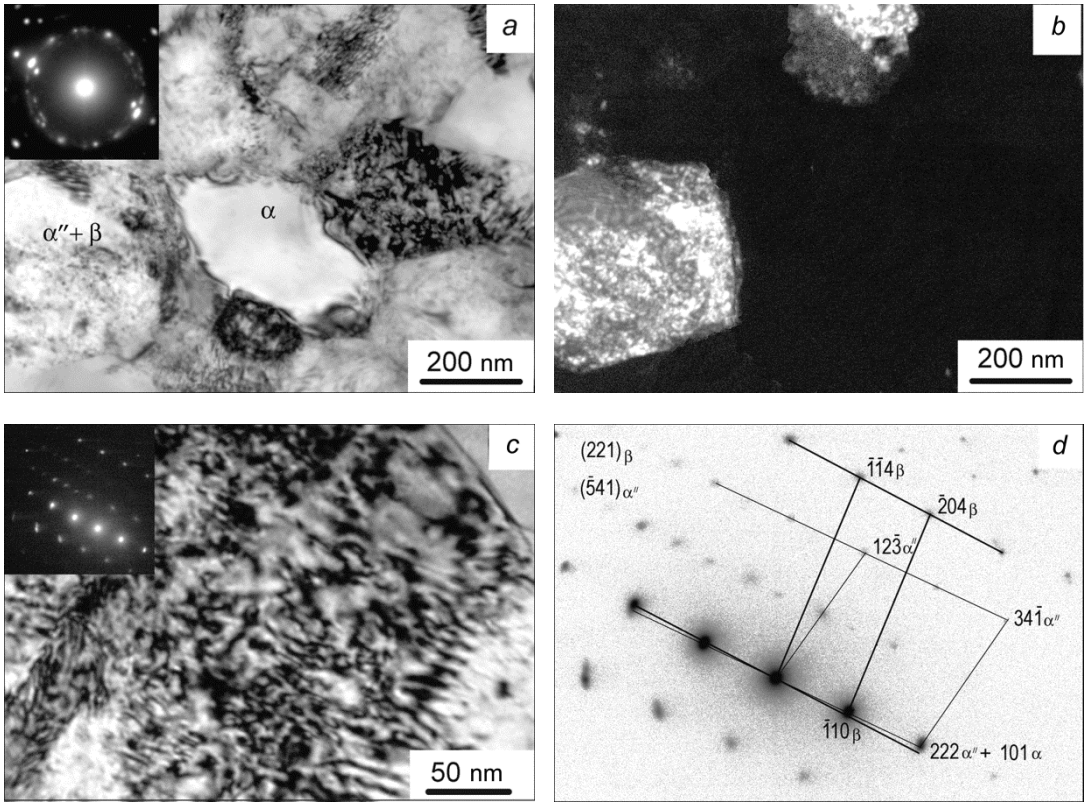

Fig. 5. Electron-microscope image of the microstructure of the VT16-0.15H alloy after hydrogen degassing: *a*) bright-field image, *b*) dark-field image in the [002]α reflection, and *c*) bright-field image of an α(α″) + β grain.

average size of the elements of the UFG structure of the VT16-0.15H alloy, determined from the dark-field image, is (0.26 ± 0.12) μm, i.e., it differs insignificantly from the average size of the elements of the structure of the VT16 alloy obtained after five pressing cycles. Consequently, the presence of hydrogen in solid solution makes it possible to decrease the number of pressing cycles in the formation of a UFG structure in the VT16 alloy.

Above, we noted the need for degassing of hydrogen from titanium alloys due to its embrittling effect. We performed hydrogen degassing from the VT16-0.15H specimens with UFG structure by annealing at 874 K for 30 min. After such an anneal, the hydrogen content in the specimens dropped to a concentration corresponding to the technical requirement (~0.004 wt%, which we will refer to below as the VT16-0.004H alloy), but the UFG structure was preserved. Figure 5 presents an electron-microscope image of the UFG structure of the alloy after hydrogen degassing. In the bright-field image (Fig. 5*a*) it can be seen that the grain boundaries of the UFG structure after degassing become more distinct. The average size of the elements of the grain-subgrain structure, determined from the dark-field image (Fig. 5*b*), after hydrogen degassing practically did not change and stood at (0.25 ± 0.16) μm. In the UFG structure after degassing there are two types of grains: grains having lamellar morphology with transverse dimension of the platelets equal to 5–10 nm (Figs. 5*a* and *c*), and grains free of precipitation with a low density of dislocations. The fraction of grains with lamellar structure here is ~70%.

X-ray structural analysis showed that the diffraction pattern of the UFG structure of the VT16-0.15H alloy after degassing reveals a substantial drop in the intensity of the reflections of the β-phase (Fig. 1, curve *4*), which attests to the development during degassing of a β→α transformation. The magnitude of the microdistortion of the crystalline lattice of the β-phase changed insignificantly and stood at $2.0 \cdot 10^{-3}$. The lattice parameter of the β-phase as a result of hydrogen degassing decreased to 0.3242 nm, which is indicative of the active development of diffusion and redistribution of the doping elements in the alloy. Moreover, the diffraction pattern of the UFG structure of the alloy

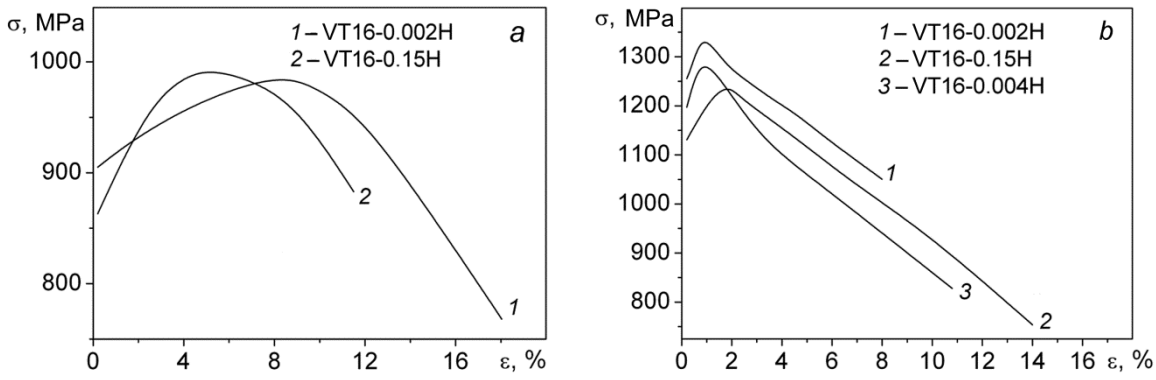

Fig. 6. Tensile curves at room temperature of the VT16 and VT16-0.15H alloys: *a*) the CG state and *b*) the UFG state.

after degassing reveals a substantial broadening of some peaks of the α-phases. A similar analysis of the diffraction pattern showed that, besides the α- and β-phases, the α″-phase is present in the alloy. The magnitudes of the microdistortions of the crystalline lattices of the α- and α″-phases are, respectively, $1.3 \cdot 10^{-3}$ and $2.8 \cdot 10^{-3}$. The presence in the UFG structure of the α- and α″-phases after degassing is in agreement with the presence in the electron-microscope image of the structure of two types of grains. Analysis of the electron diffraction pattern showed that the grains not containing precipitations are grains of the α-phase. These can be grains of the α-phase arising during pressing. Grains with lamellar morphology contain the α″- and β-phases (Figs. 5*c* and *d*). Such grains in the structure can be formed during hydrogen degassing and cooling from the degassing temperature as a result of the β→α transformation and precipitation in the grains of the β-phase and the α″-phase in the form of platelets. Hence, the more stressed state of the α″-phase found in the grains with lamellar structure is due to the fact that the α″- and β-phases have different specific volumes, for which reason their presence in one grain gives rise to additional internal stresses.

Figure 6 displays tensile curves at room temperature of the VT16 and VT16-0.15H alloys in the coarse-grained (CG) and UFG states. It can be seen that in general two stages are observed: a strengthening stage and a stage characterized by weakening of the stress. Hydrogenation of the coarse-grained VT16 alloy to 0.15 wt% leads to a decrease in the duration of both stages of deformation (Fig. 6*a*). For the alloys in the UFG state, a short (per deformation, ~1%) stage of strain hardening (Fig. 6*b*, curves *1* and *3*) is characteristic. The presence of 0.15 wt% hydrogen in the UFG alloy facilitates an increase in the duration of both stages of deformation (Fig. 6*b*, curve *2*). However, the duration of the stage of strain hardening of the VT16-0.15H alloy in the UFG state remains roughly two times shorter in comparison with the corresponding value for the CG state.

The values of the strength and plasticity characteristics at room temperature of the VT16 and VT16-0.15H alloys in different structural states are listed in Table 1. It can be seen that hydrogenation of the VT16 alloy in the CG state up to 0.15 wt% has practically no effect on the value of the strength limit (σ_B), but lowers the yield point (σ_{02}) and the total strain to failure (δ). Formation of the UFG state leads to an increase of the strength characteristics of the alloy by 30–40% in comparison with the CG state, including in the presence of hydrogen in solid solution. At the same time, in the presence of hydrogen in solid solution in the VT16-0.15H alloy in the UFG state, and also in the CG state, there is observed a lowering of the strength characteristics. Such a decrease of the strength characteristics of the VT16 alloy in the CG and the UFG states can be due to a weakening of the β-phase caused by an increase of its volume fraction and a decrease of the content of doping elements in it. Moreover, the lowering of the σ_{02} values in the VT16-0.15H alloy in the CG and UFG states is in agreement with observations *in situ* [15], according to which the presence of hydrogen in solid solution in Ti, Nb, V, and Fe, and in alloys based on them promotes the nucleation of dislocations and increases their mobility. The increase in the strength characteristics of the UFG alloy after degassing is apparently due not only to an increase in the strength of the β-phase, but also to the formation in the majority of grains of a lamellar structure. It is well known [16] that the resistance to deformation of the lamellar structure of titanium alloys is higher in comparison with that of the globular structure.

TABLE 1. Mechanical Properties of the Titanium Alloys VT16 and VT16-H in the CG and UFG States at Room Temperature

Material	d, μm	$\sigma_{02} \pm 50$, MPa	$\sigma_B \pm 50$, MPa	$\delta \pm 1$, %
CG VT16-0.002H	27	905	987	18
CG VT16-0.15H	27	874	992	11
UFG VT16-0.002H	0.23	1256	1335	8
UFG VT16-0.15H	0.26	1131	1234	14
UFG VT16-0.004H	0.25	1197	1286	11

It is clear from a comparison of the strength characteristics of the UFG alloy VT16 in different structural states that the structure obtained as a result of five pressing cycles has large values of σ_{02} and σ_B and a small value of δ. This is apparently due to the presence in the structure of higher internal stresses in comparison with the structure obtained using reversible hydrogenation. It is well known [17] that high internal stresses in UFG materials hinder the movement of dislocations. Two consequences of this are an increase in the strength characteristics of the UFG structure and a decrease in the uniform and overall deformation of the material. Hence, if it is taken into account that hydrogen, being found in solid solution, promotes the nucleation of dislocations and increases their mobility, then a growth in the values of δ of the VT16-0.15H alloy in the UFG state in comparison with the corresponding values for the UFG state of VT16 becomes comprehensible.

CONCLUSIONS

Preliminary hydrogenation to a concentration of 0.15 wt% makes it possible to lower by more than a factor of 2 the magnitude of the plastic deformation necessary for formation in the VT16 alloy, by pressing with a change in the deformation axis, of the UFG state with average size of the elements ~0.25 μm. During pressing at 1023 K and 923 K, there takes place in the titanium alloy VT16-0.15H (i.e., the VT16 alloy containing 0.15 wt% hydrogen) containing the α'', α, and β phases in its initial state, the complete phase transformation $\alpha'' \rightarrow \beta \rightarrow \alpha$ and formation of a two-phase $\alpha+\beta$ UFG state with high – up to 42 vol.% – content of the depleted β-phase. Under conditions of subsequent hydrogen degassing at 873 K, such processes are observed in the UFG structure as the phase transformation $\beta \rightarrow \alpha'' \rightarrow \alpha$ and a redistribution of the doping elements promoting the formation in the β-grains of a thin lamellar $(\beta+\alpha'')$-structure and preservation of the high level of the strength properties of the UFG VT16 alloy.

This work was performed within the scope of the Program of Basic Scientific Research of Academies of Sciences during the timeframe 2013–2020, Direction Sh-23, using equipment of the Shared Use Center NANOTECH of the Institute of Strength Physics and Materials Science of the SB RAS and the Materials Science Center for Collective Use of Tomsk State University.

REFERENCES

1. R. Z. Valiev, Y. Estrin, Z. Horita, *et al*., Mater. Res. Lett., **4**, No. 1, 1–21 (2017).
2. H. Yilmazer, M. Sen, M. Niinomi, *et al*., RSC Advances, **6**, 7426–7430 (2016).
3. A. É. Svirid, N. N. Kuranova, A. V. Lukyanova, *et al*., Russ. Phys. J., **61**, No. 9, 1681–1686 (2018).
4. B. B. Straumal, A. R. Kilmametov, Yu. Ivanisenko, *et al*., Adv. Eng. Mater., **17**, No. 12, 1835–1841 (2015).
5. Ke Hua, Jinshan Li, Hongchao Kou, *et al*., J. Alloys Compd., **671**, 381–388 (2016).
6. G. P. Grabovetskaya, I. V. Ratochka, I. P. Mishin, *et al*., Russ. Phys. J., **59**, No. 1, 109–115 (2016).
7. V. E. Panin, V. E. Egorushkin, A. V. Panin, and A. G. Chernyavskii, Fizich. Mezomekh., **19**, No. 1, 31–46 (2016).
8. S. A. Akkuzin, I. Yu. Litovchenko, A. N. Tyumentsov, and V. M. Chernov, Russ. Phys. J., **62**, No. 4, 698–704 (2019).

9. N. A. Popova, E. L. Nikonenko, N. R. Sizonenko, and N. A. Koneva, Russ. Phys. J., **60**, No. 4, 615–623 (2017).
10. H. C. Kou, H. L. Zhang, Y. D. Chu, *et al*., Acta Metall. Sin., **28**, No. 4, 505–513 (2015).
11. A. A. Il'in, B. A. Kolachev, and V. K. Nosov, Hydrogen Technology of Titanium Alloys [in Russian], National University of Science and Technology "MISIS" Publishing House, Moscow (2002).
12. Yanxu Zong and Kunyao Wu, Mater. Sci. Eng. A, **703**, 430–437 (2017).
13. I. P. Mishin, G. P. Grabovetskaya, O. N. Zabudchenko, and E. N. Stepanova, Russ. Phys. J., **57**, No. 4, 423–428 (2014).
14. M. V. Mal'tsev and N. I. Kashnikov, Fiz. Met. Metalloved., **45**, No. 2, 426–428 (1978).
15. J. V. Robertson, Eng. Fract. Mech., **68**, 671–692 (2001).
16. E. W. Collings, Physical Metallurgy of Titanium Alloys, American Society for Metals, Cleveland (1984).
17. Panin V. E. and Egorushkin V. E., Phys. Mesomech., **12**, No. 5–6, 204–220 (2009).